Essential Readings in Light Metals: Aluminum Reduction Technology.
Edited by Geoff Bearne, Marc Dupuis and Gary Tarcy.

Alcoa STARprobe™

Xiangwen Wang, Bob Hosler, Gary Tarcy
Alcoa Primary Metals, Alcoa Inc., USA

Keywords: Electrolysis, aluminum smelting, aluminum reduction, analysis method, differential thermal analysis, temperature, superheat

Abstract

Alcoa STARprobe™ is a probe device/system used to measure cryolitic bath properties including **S**uperheat, **T**emperature, **A**lumina concentration, and cryolite **R**atio (acidity), **STAR**, all together in real time for active pot control. The proprietary measurement principle is based on differential thermal analysis (DTA). This paper shows the fundamentals of operation along with the correlation of all the analysis with the accepted methods of XRD and pyrotitration for acidity, thermocouples for Bath Temperature and LECO and XRF analysis for alumina. The timing of the measurement will be shown to be equal to the traditional methods and the reliability (including reusable use of the probes) will also be described.

Introduction

The efficiency of aluminum smelting cells relies on sophisticated control in maintaining cell's thermal and material balances by regulating resistance, bath chemistry, and alumina feed. A good control of the cells is dictated by reliable and accurate measurement of key cell's operating parameters, i.e. cell (bath) temperature and electrolyte chemistry (cryolite ratio and alumina concentration). Traditionally, bath temperature measurement, bath sampling, and its subsequent analysis are usually carried out separately by different crews and sometimes at different times.

Bath temperature is usually measured using a thermocouple at a frequency of about one per day. This batched process is carried for a whole room or line. Bath compositional analysis is also a batch process that comes from sampling the individual cells, preparing the individual samples (grinding to a suitable particle). Bath analysis is a lengthy process even if some of the preparation and analysis is robotically automated in some modern smelters. Depending on the number of cells, it will take from 6 to 24 hours before results are known and corrective actions can be taken. This separate arrangement of measurements and delay in obtaining results is due to the fact that there are no better measurement options.

The drawbacks of the lengthy and tedious temperature and bath sampling/analysis are obvious: When the bath samples are being processed and analyzed, the electrolysis cells are continuously operated and their bath temperature and cell chemistry are dynamically changing due to the variation of power and material input. Control decisions in both material (chemicals) and energy (voltage/resistance) input have to be made primarily relying on old information and empirical guessing at the "current" cell condition. And this "current" cell condition may be significantly different from the "real" cell condition due to a lot of unknown factors during the period. Consequently, the inability to measure cell temperature and real time bath chemistry inherently results in poor cell control that is often either under or over the target conditions. This under- and over-control of operating target leads to sub-optimal cell performance in current efficiency and energy efficiency. Another issue with the bath sampling and lab analysis procedure is the high probability of information mix-up which will also lead to an inappropriate control action. Bath samples are taken from many electrolysis cells. These samples must be kept in order and numerically tracked through the lengthy process of preparation and analysis. Every time the sample is handled, there is a possibility of sample mix-up and possible sample contamination.

In addition to drawbacks of the conventional measurement methods, there is also lack of some key bath physicochemical information, such as liquidus temperature that is critical to efficient operation. Some advanced measurement methods have been a subject of study in the past decades (1, 2). The commercially available measurement tool by Electronite, made it possible to utilize measured bath superheat for active pot control (3, 4). Though it was a step forward from the traditional method, it never reached large scale application across aluminum smelters because:

1. The consumable and expensive probe tip could often not be justified for routine pot control use.
2. Incomplete information from the measurement. The liquidus (or superheat) can be a function of bath chemistry (ratio or %XS AlF_3) and/or alumina concentration. Lack of information with respect to the cause for an undesirable liquidus temperature could lead to very different control decisions based on the assumptions made regarding the cause. This in turn could result in inefficient operation if not disastrous consequences.

To effectively control an operating cell and to achieve its maximum efficiency, energy state, chemical state, and state of control should be known. These states are represented by core parameters including cryolite ratio (%XS AlF_3), temperature, superheat and concentration of alumina. This paper presents Alcoa STARprobe™, an advanced measurement device developed as a real time analytical tool for measuring the necessary cell information and then instantly supplying the information to the host computer for control decisions.

Alcoa STARprobe™ is a measurement tool for use in the potroom. It measures and gives bath **S**uperheat, bath **T**emperature, **A**lumina concentration in bath and cryolite **R**atio (excess AlF3) in a single measurement. It also instantly transmits the results to a host computer through wireless communications in the potroom. This procedure unites the conventional processes of temperature measurement and bath sampling-analysis into one on-line measurement, simplifies and greatly shortens the process and time space from measurement/sampling to pot control decision. The pot control decision can therefore be based on the real time

cell conditions rather than those from few hours ago or from as long as 12 or 24 hours ago.

Theoretical Background

Cryolitic Melt Cooling Characteristics

For simplicity, Na_3AlF_6 – AlF_3 binary phase system shown in Figure 1 is used for discussion.

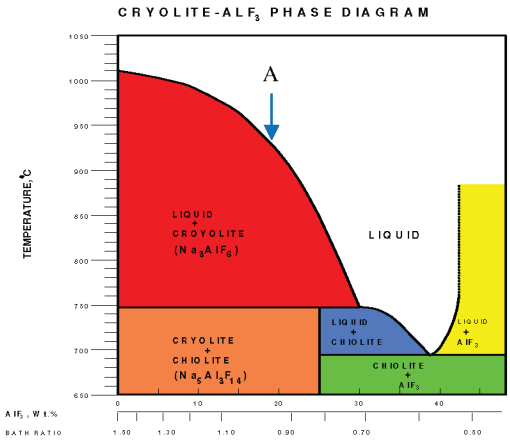

Figure 1: Na_3AlF_6-AlF_3 phase diagram.

When a cryolitic melt is cooled from liquid state to a solid state, it will go through several phase transformation/changes. For example as melt A starts to cool from its liquid state down to its liquidus (melting) temperature (~960°C), solid cryolite starts to form and the remaining liquid will have an increased AlF_3 concentration. This will continue changing along phase diagram liquidus line (the red region in the graph):

$$\text{Liq. Bath} \rightarrow Na_3AlF_6(s) + \text{Liq.(var. XS } AlF_3) \quad (1)$$

As the temperature is cooled down further to its per-eutectic temperature, solid chiolite forms (the blue region in the graph):

$$Na_3AlF_6(s) + AlF_3(l) \rightarrow Na_5Al_3F_{14}(s) \quad (2)$$

As the temperature cools further, the liquid will transform into solid leaving behind liquid at increasing AlF_3:

$$\text{Liq.bath} \rightarrow Na_3AlF_6(s) + Na_5Al_3F_{14}(s) + \text{Liq.(var. XS } AlF_3) \quad (3)$$

Finally, when the temperature reaches the eutectic (intersection of the blue green and yellow regions) there is no more remaining liquid:

$$\text{Liq. bath} \rightarrow Na_5Al_3F_{14}(s) + AlF_3(s) \quad (4)$$

As can be seen from the phase diagram, each phase transformation of cryolite components occurs at specific temperature regions, and component phase changes are accompanied by heat release (ΔHi). The amount of heat release is directly proportional to the amount of the component.

Differential Thermal Analysis (DTA)

The principle of DTA in material characterization is illustrated in Figure 2. Any material which goes through phase transformation associated with energy (heat) release, can be analyzed by DTA. The sample is typically placed in a sample cup/container in parallel with a reference material. When the sample together with the reference is heated up or cooled down, the heat adsorption or release due to phase transformation can be reflected through the temperature difference (TC1-TC2).

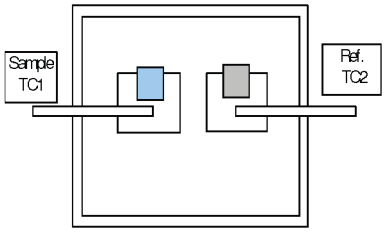

Figure 2: Differential thermal analysis (DTA) for materials characterization.

If a cryolitic melt (shown in the phase diagram Na_3AlF_3 – AlF_3 in Figure 1), is placed in DTA (Figure 2) and cooled against an ideal reference in a control environment, cryolite (Na_3AlF_6) and chiolite ($Na_5Al_3F_{14}$) may be easily determined. Shown in Figure 3 are three different compositions cooled from their melting state.

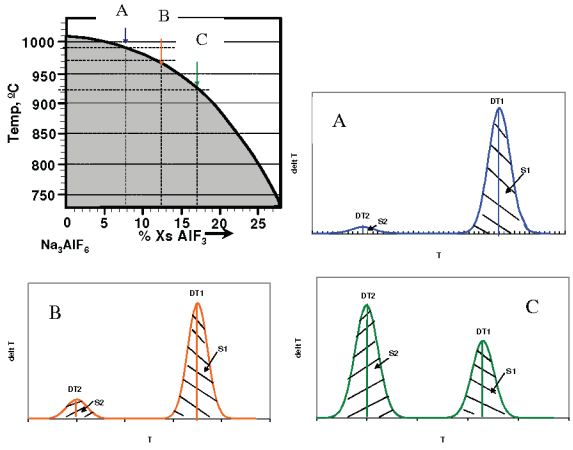

Figure 3: Typical DTA patterns of cryolitic melts with three different %XS AlF_3 or bath ratio (A, B, and C).

Three distinct patterns, specifically, the peaks of delta T for cryolite and chiolite appear. The cryolite ratio (NaF/AlF_3) or %XS AlF_3 is directly related to the heat of release during the phase transformations and therefore the magnitude of delta T:

$$\%\text{XS AlF3} = f1[\Delta H_{AlF3/Na5Al3F14}/(\Delta H_{AlF3/Na5Al3F14} + \Delta H_{Na3AlF6})] = f2[S2/(S1+S2)] = f3[DT2/(DT1+DT2] \quad (5)$$

The Alcoa STARprobe™ was developed based on the principle of DTA so that those unique cooling characteristics can be clearly revealed and the cryolitic ratio accurately determined (5, 6). The ratio result can be known after carrying out a few simplified steps:

- First insert probe tip in molten bath to equilibrate with bath temperature in an electrolysis cell
- Take probe tip out of molten bath and allow it to cool
- STARprobe™ analyzes the cooling curve and reports the results.

Results and Discussion

The current Alcoa STARprobe™ system is shown in Figure 4. The STARprobe consists of four major components: 1.) reusable probe tip, 2.) portable probe stand/lance to fit various smelters for measurement, 3.) electronics which acquire temperature data, analysis and carryout wireless communications, and 4.) STARprobe™ program which performs all the necessary tasks during measurement.

Figure 4: Alcoa STARprobe™ measurement system.

Probe Tip Development

The probe tip and the material used in constructing/making the probe tip are considered to be critical in effectively revealing cryolite cooling characteristics in a repeatable fashion. Another important consideration is the temperature measurement (7, 8). The type K thermocouples used in the probe tip offer accurate temperature (better than ±0.4%), fast response time to temperature and, most important of all, being able to withstand molten bath for multiple uses. One of the probe tip designs is presented and shown in Figure 5 a.

A typical cooling curve of a molten cryolitic bath from a molten sate to a solid state in the probe tip is shown in Figure 5 b and c.

Bath Temperature and Liquidus:

The probe tip is designed so the liquidus temperature is clearly revealed with no supercooling. As an example, Figure 6 shows bath liquidus temperatures for three typical cryolite ratio conditions, i.e. bath ratio of 1.20, 1.10, and 1.00, a range representing aluminum smelting conditions.

Table I shows the typical accuracy for determining liquidus temperature when electrolyte composition was maintained constant. Each measurement was repeated ten times and each time it started with a different bath temperature. The standard deviation of the measured liquidus was 0.43°C. Since bath temperature was not kept constant, the superheat therefore changed accordingly.

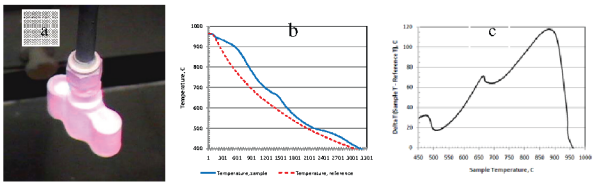

Figure 5: a.) The probe tip (with molten cryolitic bath) is being cooled, b.) Temperature of bath sample and reference, and c.) differential temperature as a function of sample temperature.

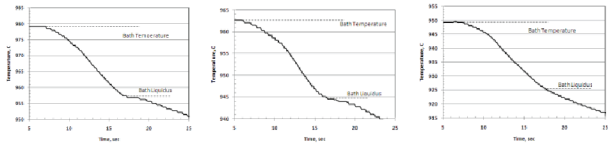

Figure 6: Cryolitic electrolyte temperature and liquidus as revealed by the probe for three ratio conditions: a.) 1.20, b.) 1.10, and 3.) 1.00 from left to right.

Table I Bath Temperature and Liquidus by STARprobe™

Test No.	Temperature, C	Liquidus, C	Superheat, C
1	961.5	944.8	16.7
2	965.3	944.0	21.3
3	962.9	944.6	18.3
4	960.3	945.1	15.2
5	967.3	944.0	23.3
6	964.8	944.5	20.3
7	965.3	944.0	21.3
8	969.3	944.8	24.5
9	967.4	944.8	22.6
10	963.9	944.0	19.9
Avg:	**964.6**	**944.5**	**20.1**

Bath superheat was compared with a commercially available method. Figure 7 shows comparison of results obtained in a smelter setting. Each point represents an operating cell: The results of Alcoa STARprobe™ agree well with the "reference" method. The difference between the two methods as observed is believed to be mainly due to 1.) different algorithms in determining the "true" liquidus temperature at its "inflection" point, 2) natural variation of smelting conditions especially when there is feeding and 3) the fact that the two were not measured at the "exactly" same time.

Cryolite Ratio:

As illustrated in Figure 3, the magnitude of heat released from the cryolite and chiolite phase transformation is a function of their initial constituents. Figure 8 shows how the STARprobe™ measures bath ratio by first utilizing the cooling characteristics bath with different starting ratios. When bath ratio increases, the liquidus temperature increases, the differential temperature for cryolite phase formation (marked as peak 1) increases, and the differential temperature for chiolite phase formation (peak 2) decreases.

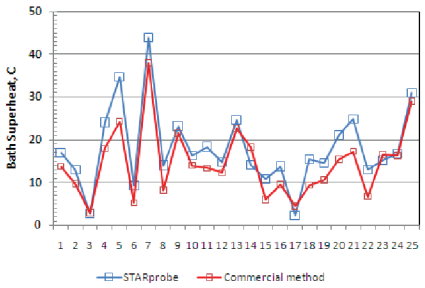

Figure 7: Bath superheat as measured by STARprobe and commercially available method in a smelter setting.

With a proper analysis of these cooling characteristics the ratio is determined. Shown in Figure 9 is the bath ratio determined using the key cooling curves characteristics. The probe tip produces a non-biased response to the ratio variation in the range of interest. The maximum variance (3 measurements at each ratio condition) was 0.00015 and maximum difference between the target and measured ratio was 0.012.

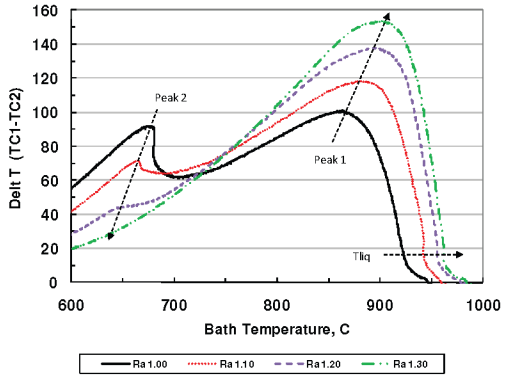

Figure 8: Differential temperature as a function of bath temperature at different ratio conditions.

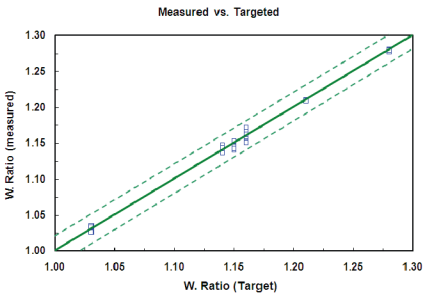

Figure 9: Bath ratio as determined using key cooling characteristics in STARprobe™.

Alumina Concentration:

Typical alumina concentration in smelting bath ranges from a low 1.5 to as high as 7.0wt%. The relatively low concentration of alumina represents a small amount of heat release when alumina crystallizes out of a cooling/freezing bath. This small amount of heat release means limited representation on the cooling curve with respect to the other phase transformations. The sensitivity of detecting the heat release is therefore more limited. Nevertheless, as shown in Figure 10, the probe tip is able to detect varied alumina concentration in bath. When alumina concentration increases, the bath liquidus decreases. Most important of all, there is another peak (heat of release) between 800 and 900°C, and this peak increases when alumina concentration in bath gets higher. These two major features plus other features allow the alumina concentration in bath to be measured by the STARprobe™ as shown in Figure 11. Like bath ratio, the STARprobe™ has a non-biased response in measuring %alumina in bath but with some reduced accuracy compared to ratio. The maximum variance was 0.14% and maximum difference between targeted and measured value was 0.66%.

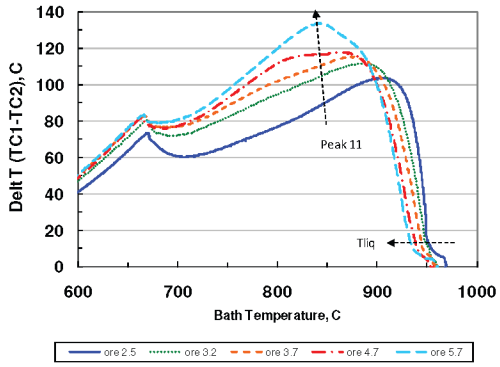

Figure 10: Characteristics of alumina crystallization as a function of alumina concentration in bath.

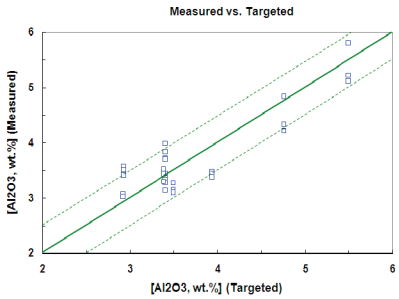

Figure 11: %Alumina as measured by STARprobe™ using key cooling alumina characteristics.

Environmental Impact:

The probe tip is cooled in the ambient environment after it equilibrated with bath temperature when removed from the pot. Figures 12 to 14 show the potroom ambient conditions on probe cooling have little impact on the measurement of liquidus temperature, ratio and alumina concentration due to the differential nature of the measurement. Under three ambient temperature conditions, i.e., >150°F (65°C), 78°F (25°C), and <-150°F (-101°C), the following results were obtained:

- For liquidus: No significant impact was observed. Standard deviations at the two temperatures or electrolyte conditions) were respectively 1.13 and 0.98°C
- For ratio: the standard deviations at two ratios were found to be: 0.0123 and 0.043.

- For alumina: the standard deviations at two levels were found to be: 0.24% and 0.13%.

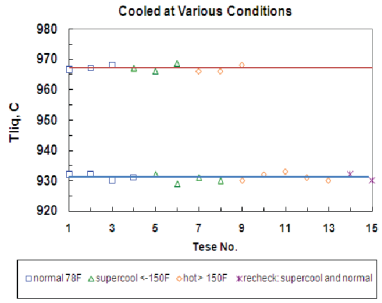

Figure 12: Impact of ambient temperature on liquidus.

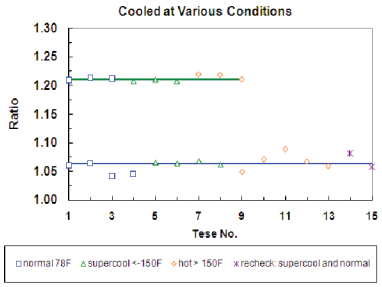

Figure 13: Impact of ambient temperature on bath ratio.

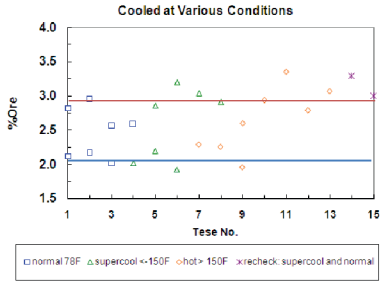

Figure 14: Impact of ambient temperature on alumina.

Alcoa STARprobe™ System

Alcoa STARprobe™ system was designed and built by incorporating the core probe described in the previous section. It has evolved from early MS-DOS™ based in early 2000 to the current version. It is a portable and yet fully integrated system for making measurement on cells of different technologies:

- PDA or tablet PC based electronics which satisfy special potroom conditions (high magnetic field, high ambient temperature, and highly dusty environment).
- User friendly and yet robust running program with simple graphical user interface (GUI) which is targeted to all audiences from pot operators to engineers.
- Wireless data management which takes advantage of secured wireless technology in both acquiring temperature data and transferring results to the computer server. This makes it possible for real time measurement and pot control.
- Self adjustable stand/lance and probe tip assembly which fits all cell technologies (pre-baked or Soderberg, floor or deck plate based) for an easy measurement.

Figures 15 and 16 show photos of PDA and tablet PC based STARprobe™ systems. The major difference between the two is that PDA based is a standalone unit while a single tablet PC based unit can control up to two probes (also shown in Figure 4). Figure 17 further illustrates the tablet based STARprobe™ measurement cycle: two probes are inserting in tap hole of each cell in measurement, temperature data transfers to tablet via wireless, the tablet processes the measured data and transfers the results to computer server via the wireless network. The computer server gives control instructions to the pot to complete the control cycle.

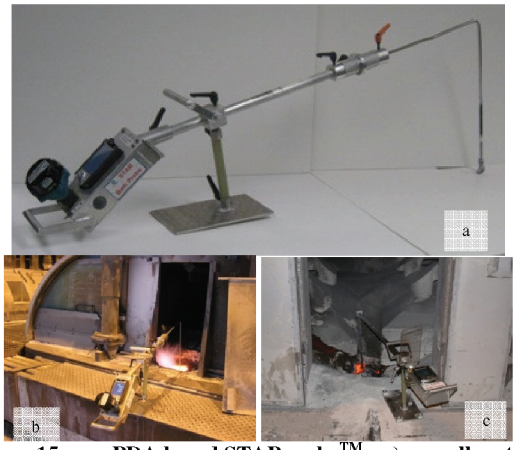

Figure 15: PDA based STARprobe™: a.) overall system, b. and c.) unit was in measurement on two different cells.

Figure 16: Tablet PC based STARprobe™ is being used.

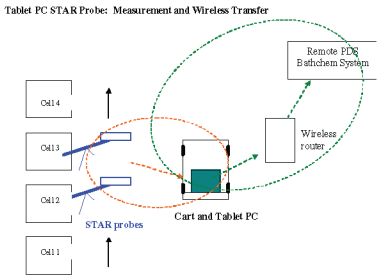

Figure 17: Schematic showing the STARprobe™ measurement and data management in a potroom setting.

Measurement Time:

Since the probe tip is reused, a complete measurement requires a few steps from setting probe tip in bath, taking probe tip out of bath to cool, to put the probe tip back to the pot to reheat for dumping bath out of the probe for next new measurement. When

used continuously, average time is just under 4 minutes to complete the measurement cycle.

STARprobe™ Repeatability/Resolution

Under Controlled Lab Conditions:

To determine repeatability or variability of liquidus, three repeated measurements were carried for each bath composition, temperature was intentionally changed at each composition, and 16 bath compositions were studied over a period of time. This was also to determine if there is any possible chance of supercooling in determining liquidus. Figure 18 shows the bath temperature and liquidus of three measurements at each cryolite composition. The bath temperature ranged from a low of 935°C to a high closed to 1000°C while the liquidus ranged from a low of 910°C to a high of 980°C.

As shown in Table II, for a 16 bath (ratio) compositions, the average standard deviation for the measured bath ratio is 0.0085 (max. 0.02 and min 0.00), while for liquidus, the standard deviation is 1.1°C (max 2.8 and min 0.2°C. The variability of the liquidus at each bath composition is independent of bath temperature variation or the difference between temperature and liquidus, indicating there is no apparent supercooling in measurement.

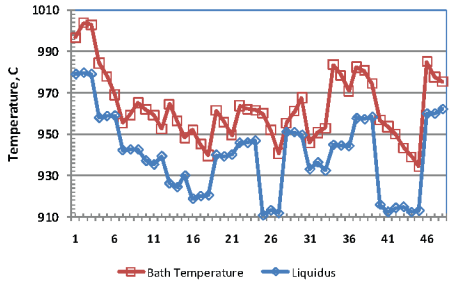

Figure 18: Bath temperature and liquidus of 3 repeated measurements at electrolyte composition.

Examples Measured in Industrial Smelting Cells:

Three repeated STARprobe™ measurements were carried out for 10 cells, and 3 bath samples were also taken at the same time. Bath samples were then analyzed with conventional analytical method. Figure 19 shows the bath temperature and liquidus of all measurements, and Figure 20 shows the ratio measured by STARprobe and analyzed by XRD method. The variance in ratio is comparable: an average of 0.00012 of sampling/XRD vs. 0.00010 by STARProbe.

Table II Repeatability (Variance) of Bath Liquidus

		Stddev
(Tb – Tliq), C	Average	10.5
	Max	19.3
	Min	2.2
Liquidus, C	Average	1.07
	Max	2.82
	Min	0.19
Bath Ratio	Average	0.0085
	Max	0.0204
	Min	0.0014

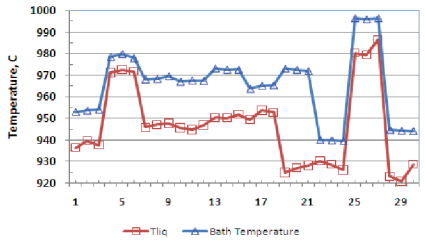

Figure 19: Bath temperature and liquidus as measured by STARprobe™ in a repeated fashion.

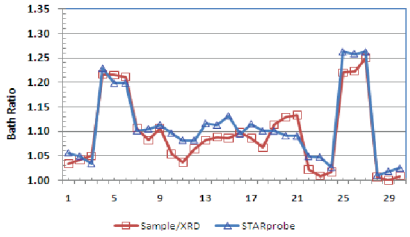

Figure 20: Bath ratio as measured by STARprobe™ and analyzed by sampling/XRD.

Summary

Alcoa STARprobe™ is designed and developed to measure key cell parameters, i.e. bath superheat, temperature, alumina and ratio for real time active pot control. This paper presents its development, working principles as well as results in comparison with traditional methods. It is being used across Alcoa smelters, replacing the conventional sampling methods.

Acknowledgment

The development of the Alcoa STARprobe™ was only possible with the efforts of many departments. The authors, with deepest appreciation, wish to acknowledge Geff Wood for supporting and supplying talents of his department in coding the STARprobe™ program and choosing the proper electronics, without of which there would not be a STARprobe.

References:

1. Y.R Gan et al: "Multifunction Sensor for Use in Aluminum Cells", TMS Light Metals, 1995, p233.
2. P Verstreken and S Benninghoff: "Bath and Liquidus Temperature Sensor for Molten Salts", TMS LM, 1996, p437.
3. M. P. Taylor and J. J. Chen: "Applying Control Principles to Superheat", 1st Superheat user Meeting, 19th – 23rd, March 2005, South Africa.
4. P Verstreken: "Review of 9-box Control – How can we improve", 1st Superheat user Meeting, 19th – 23rd, March 2005, South Africa.
5. C. Bates: US Patent 6,220,748, expires 1/15/2019.
6. B Hosler et al: US Patent 6,942,381, expires9/25/2023.
7. D. J Madsen: "Temperature Measurement and Control in Reduction Cells", TMS Light Metals 1992, p453.

8. X. Wang et al: "Paradox in cell Temperature Measurement Using Type K Thermocouple", TMS Light Metals, 2006, p279.

Recommended Reading

Adkins, E.M., and J.A. Murphy. Operating experience with a digital computer at NSA's Kentucky aluminum reduction plant (1973, Vol.1, pp. 27–38).

Al Zarouni, A., et al. Towards eliminating anode effects (2011, pp. 333–337).

Bearne, G., and D. Whitfield. Improving reduction cell metal level measurement and control (2005, pp. 413–418).

Berezin, A.I., et al. FMEA-based expert system for electrolysis diagnosis (2005, pp. 429–434).

Bohlin, U. Computer control of aluminum electrolysis at granges aluminum employing "normalized voltage" (1973, Vol.1, pp. 39–56).

Dando, N.R. Using fume duct temperature for minimizing open holes in pot cover (2004, pp. 245–248).

Entner, P.M., and G.A. Guomundsson. Further development of the temperature model (1996, pp. 445–449).

Gan, Y.R., Z.S. Gao, and A.L. Zhang. Multifunctional sensor for use in aluminum cells (1995, pp. 233–241).

Gao, Y., et al. Human factors in operational and control decision making in aluminium smelters (2011, pp. 605–609).

Haverkamp, R.G. Eliminating anode effects (1999, pp. 285–288).

Huni, J.P.R. A-275 -- individual anode control (1987, pp. 199–202).

Iffert, M., M. Skyllas-Kazacos, and B. Welch. Challenges in mass balance control (2005, pp. 385–391).

Jentoftsen, T., et al. Correlation between anode properties and cell performance (2009, pp. 301–304).

Kvande, H., J.J.J. Chen, and W.E. Haupin. Minimizing energy consumption through optimizing alumina concentration in the bath of Hall-Héroult cells (1994, pp. 429–440).

Madsen, D.J. Temperature measurement and control in reduction cells (1992, pp. 453–456).

Majid, N., et al. Detecting abnormalities in aluminium reduction cells based on process events using multi-way principal component analysis (MPCA) (2009, pp. 589–593).

Manaktala, S. C. Process control techniques for reduction cell operation (1971, pp. 165–174).

Meghlaoui, A., and N. Aljabri. Aluminum fluoride control strategy improvement (2003, pp. 425–429).

Meyer, H.J., and D. G. Earley. Anode effect prediction (1986, pp. 365–376).

Moen, T., J. Aalbu, and P. Borg. Adaptive control of alumina reduction cells with point feeders (1985, pp. 459– 469).

Navarro, P., et al. A new anode effect quenching procedure (2003, pp. 479–486).

Neto, E.S.D, L.V.M. Ivo, and O.M. Guzzon. Cell operation improvement using wireless human-machine interfaces (2005, pp. 399–405).

Radulescu, C., et al. Method for automated adjustment of alumina feeding times in smelting pots (2006, pp. 297–300).

Ramones, J., et al. CVG-venalum potline control and supervisory integrated system VEN-PCSIS (2010, pp. 507–512).

Ritter, C.M., L.F.R. Neves, L.V.M. Ivo, and J.H.S. Trigueiro. Distribution aspects in reduction line control systems (2000, pp. 271–276).

Rodnov, O.O., P.V. Poliakov, A.I. Berezin, P.D. Stont, and I.V. Mezhubovsky. Estimation of a technological condition of the aluminium reduction cells on the basis of its daily energy balance (2003, pp. 457–468).

Rolland, W.K., et al. Haldris -- an expert system for process control and supervision of aluminium smelters (1991, pp. 437–443).

Schneller , M. In situ aluminum cell control (2010, pp. 563–568).

Stam, M., et al. Development of a multivariate process control strategy for aluminium reduction cells (2009, pp. 311–315).

Stam, M., et al. Common behavior and abnormalities in aluminium reduction cells (2008, pp. 309–314).

Steingart, D.A., et al. Wireless measurement of duct temperatures on aluminum smelting pots: Correlation to roofline HF concentration (2008, pp. 221–225).

Tabereaux, A.T., and N.E. Richards. An improved alumina concentration meter (1983, pp. 495–506).

Tarcy, G.P., S. Rolseth, and J. Thonstad. Systematic alumina measurement errors and their significance in the liquidus enigma (1993, pp. 227–232).

Tessier, J., et al. Multivariate statistical process monitoring of reduction cells (2009, pp. 305–310).

Tessier, J., et al. Analysis of a potroom performance drift, from a multivariate point of view (2008, pp. 319–324).

Tikasz, L., R.T. Bui, and V. Potocnik. Expert system applied to control of aluminium smelters (1990, pp. 197–202).

Utigard, T.A. Why 'best' pots operate between 955 and 970°C (1999, pp. 319–331).

Whitfield, D., et al. Aspects of alumina control in aluminium reduction cells (2004, pp. 249–255).

Whitfield, D., et al. Metal pad temperatures in aluminium reduction cells (2004, pp. 239–244).

Wilson, M.J. Practical considerations used in the development of a method for calculating aluminium fluoride additions based on cell temperatures (1992, pp. 375–378).